Insights on in situ $MgAl_2O_4$ Formation Mechanism and its Correlation with the Corrosion Resistance of Spinel-containing Refractory Castables

E.Y. Sako, M. A.L. Braulio, V. C. Pandolfelli

The *in situ* formation of magnesium-aluminate spinel ($MgAl_2O_4$) is usually followed by a positive volumetric change and a resulting pore generation after the reaction. However, when compared to castables containing synthesized spinel grains, *in situ* spinel-forming castables usually show excellent corrosion performance in both laboratorial tests and industrial applications, even presenting such expansive reaction and apparently a more porous microstructure. Considering this scenario, the objective of the present work is to shed some light on these two main questions: a) what does really rule the *in situ* spinel formation in refractory castables, and b) if this phase formation reaction is followed by expansion and pore generation, why do spinel-forming castables present excellent corrosion resistance in industrial applications. The results suggested that the faster Mg^{2+} migration during the spinel formation led to vacancy accumulation and, consequently, to pore generation, as a direct result of the *Kirkendall* effect. Nonetheless, its performance is less affected by such mechanism then by the location of CA_6 crystals in its microstructure (as these castables are usually bonded with CAC), which results in a suitable physicochemical protection of both, the tabular alumina aggregates and the matrix.

1 Introduction

Although many academic studies and end-user reports have stated throughout the years that *in situ* spinel-forming castables present better slag resistance and longer service life in steel ladles when compared to those containing pre-formed spinel grains [1], no persuasive statements have been attained so far. Such unanswered query came again under the spotlight when other authors [2] figured out that when *in situ* spinel is formed during sintering step, the castable average pore size tends to increase. With a greater amount of large pores, the molten slag would infiltrate much easily through the microstructure, contradicting the well-known excellent slag infiltration resistance of spinel-forming refractories.

Therefore, in order to have an overall explanation, which leads to a better performance of such castables, one should at first deeply understand the main features of the reaction between alumina and magnesia and how it changes the microstructure during sintering. Since the early sixties, *Wagner, Carter* and *Nakagawa* [3–5] have been improving the theory involving the spinel formation mechanism in atomic scales, concluding that the inter-diffusion of Mg^{2+} ions from the MgO particle is much faster than the Al^{3+} counter-flux. Due to this aspect, the reaction is believed to be ruled by the so-called *Kirkendall* effect [6], which is characterized by the formation of pores in the initial location of the higher mobility component.

In alumina-magnesia refractory castables, the spinel formation ruled by the Kirkendall effect should lead to an increase in the average pore size as the magnesia grains are then gradually consumed. In addition, calcium hexaluminate ($CaO \cdot 6Al_2O_3 - CA_6$) features are barely taken into account when studying the differences in the corrosion resistance of cement-bonded castables with *in situ* or pre-formed spinel addition. Usually associated as a straightforward reaction product between alumina and CA_2, the CA_6

Eric Y. Sako, Mariana A.L. Braulio, Victor C. Pandolfelli
Federal University of São Carlos
Materials Microstructural Engineering Group
GEMM (FIRE Associate Laboratory)
13565-905 São Carlos
Brazil

Eric Y. Sako
Saint-Gobain do Brasil
Refractories Technical Department
13280-000 Vinhedo
Brazil

Corresponding author: *V. C. Pandolfelli*
E-mail: vicpando@ufscar.br

Keywords: spinel castables, in situ formation, corrosion resistance

Received: 02.11.2013
Accepted: 26.11.2013

Tab. 1 Composition in weight percent of the evaluated castables with different spinel incorporation route

Raw Material [mass-%]	AM1	AM2	AM3	AS
Tabular alumina (d ≤6 mm)	62	62	62	62
Tabular alumina (d <200 µm)	18	18	18	10
Pre-formed spinel (d <0,5 mm)	–	–	–	21
Dead-burnt MgO (d <13 µm)	6	–	–	–
Dead-burnt MgO (d <45 µm)	–	6	–	–
Dead-burnt MgO (d <100 µm)	–	–	6	–
Reactive alumina (d <4 µm)	7	7	7	–
Calcium aluminate cement	6	6	6	6
Fumed silica	1	1	1	1

Tab. 2 Chemical composition of the industrial steel ladle slag used in this work

Composition	MgO	Al_2O_3	SiO_2	CaO	MnO	Fe
mass-%	4,9	1,7	7,5	34,2	3,6	4

phase plays a relevant role in the corrosion behavior [7], mainly because its location in the microstructure strongly depends on the spinel incorporation route (synthesized or generated *in situ*) [2]. Therefore, the distinct CA_6 distribution in both castable should also be considered.

Based on these aspects, the present work aims to figure out the answers for those two main questions: a) what does really rule the *in situ* spinel formation in refractory castables, and b) if this phase formation reaction is followed by expansion and pore generation, why do spinel-forming castables present excellent corrosion resistance in industrial applications.

2 Materials and techniques

Three vibratable alumina-magnesia castables (AM1, AM2 and AM3) using dead-burnt magnesia (95 mass-% MgO, C/S = 0,37, *Magnesita Refratários S. A.*/BR) of different grain sizes (d <13, <45 and <100 µm) were selected for the *in situ* spinel formation evaluation. As shown in Tab. 1, for all of them tabular alumina (d ≤6 mm, *Almatis*/DE) was used as refractory aggregates and calcium aluminate cement (Secar 71, *Kerneos*/US) as the binder agent. Fine tabular alumina (d <200 µm, Almatis/DE), reactive alumina (CL370, d <10 µm, *Almatis*/DE) and microsilica (971U, *Elkem*/NO) comprised the matrix. The magnesia and fine alumina contents were selected considering a potential total spinel formation after the thermal treatment equal to 21 mass-% for all castables.

An additional alumina-spinel castable (AS) was designed and compared to the AM2 composition in order to evaluate the effect of the spinel incorporation method on the microstructural development of cement-bonded refractory castables (Tab. 1). For this material, besides tabular alumina as coarse aggregates, 6 mass-% of calcium aluminate cement, and 1 mass-% of microsilica, 21 mass-% of pre-formed spinel (AR78, d <0,5 mm, Almatis/DE) was added to the formulation.

The water content required for suitable casting ranged from 4,0 to 4,2 mass-%, providing good workability regardless of the MgO grain size. In order to evaluate whether the Kirkendall effect rules the spinel formation, scanning electron microscopy (SEM) images of the castables microstructure after firing at different temperatures (1000, 1150, 1300 and 1500 °C) were attained (*JEOL* JSM – 5900 lV/NL). Based on these images, pore size distribution measurements were conducted using Noran NSS 2.2 analyzer software (*Thermo Fisher Scientific*/US).

The corrosion cup-tests were carried out with cylindrical samples (50 mm × 50 mm) containing an internal hole of 20 mm diameter and 25 mm depth. After pre-firing the samples at 1500 °C for 5 h, the holes were filled in with 10 g of a high-iron steel ladle slag in order to perform the tests (the chemical composition of the industrial slag is presented in Tab. 2). The sample + slag set was then heated up to 1500 °C and the corrosion experiment was conducted for 2 h in a vertical tube furnace (HTRV100-250/18 *GERO*/DE) in air. After testing, the corroded samples were cut and the cross-sections were used for further microstructural analyses (SEM, JEOL JSM-5900 LV/NL).

3 Results and discussion

Fig. 1 schematically shows the spinel formation process controlled by the Kirkendall effect. Under the selected testing conditions, the magnesium aluminate phase is generated at the alumina particle side due to the faster Mg^{2+} diffusion. Conversely, a consequent counter-flux of vacancies takes place, leading to the so-called Kirkendall porosity where MgO was initially located. This reaction should lead to an increasing average pore size as magnesia grains are gradually consumed during heating up.

In order to evaluate this mechanism in actual castables, SEM microstructures of AM2 composition after firing at different temperatures were obtained and the average pore size (APS) in the matrix was measured for each stage (Fig. 2). According to *Zhang* and *Lee* [8], spinel formation usually takes place at roughly 1200 °C and, therefore, no APS difference should indeed be expected at 1000 °C and 1150 °C. After firing at

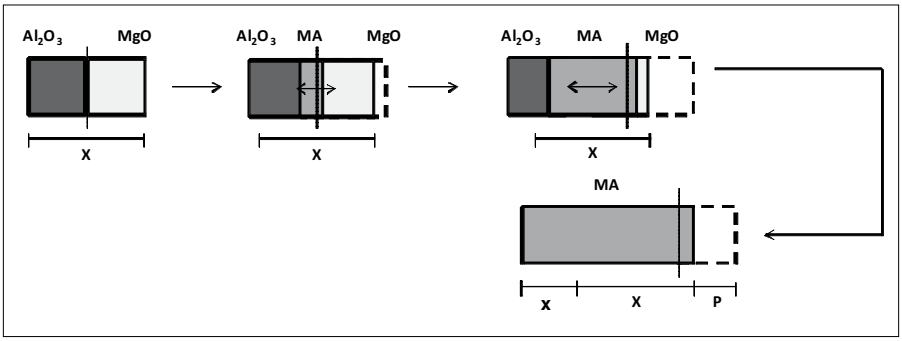

Fig. 1 Sketch of the spinel formation reaction, ruled by the Kirkendall effect

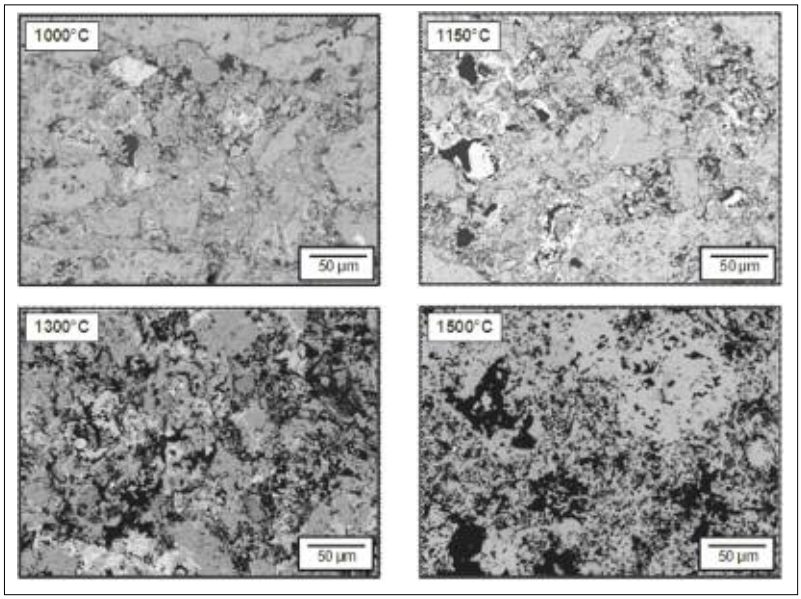

Fig. 2 SEM images of alumina-magnesia castable containing MgO <45 µm after firing at 1000, 1150, 1300 and 1500 °C (APS = average pore size in the matrix)

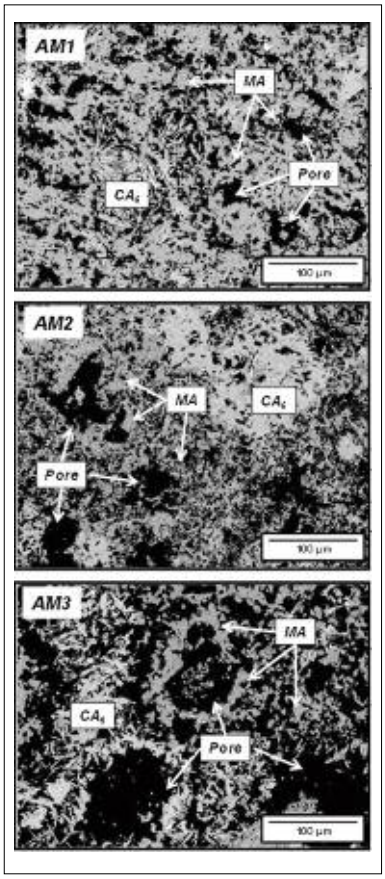

Fig. 3 Microstructure of the castables AM1, AM2 and AM3 after firing at 1500 °C for 5 h

1300 °C and 1500 °C, however, APS increased to 8 and 22 µm, respectively, indicating an indirect evidence of spinel generation ruled by Kirkendall effect. The data related to pore size presented in Fig. 2 also corroborated the results published by *Braulio et al.* [9], who detected that most of the permanent volumetric change of alumina-magnesia castables was carried out between 1300 °C and 1500 °C.

An additional aspect which reinforces that the microstructural evolution of *in situ* spinel-forming castables is controlled by the Kirkendall effect is the relationship between the average pore size after firing and the grain size. Fig. 3 shows micrographs of the castables AM1, AM2 and AM3 after firing at 1500 °C for 5 h, where large pores may be easily detected in the AM3 microstructure, whereas small ones are present in AM1. An intermediate profile was found in AM2 sample. Moreover, the presence of spinel rings around the pores are also a strong evidence that MgO was previously filling those places and, hence, the Kirkendall effect indeed controlled the spinel formation in these materials by the preferential flux of Mg^{2+} towards the surrounding alumina particles.

Nevertheless, although shedding a brighter light to the actual *in situ* spinel formation mechanism, the Kirkendall effect does not really explain the better corrosion resistance of alumina-magnesia castables when compared to alumina-spinel ones, as observed in Fig. 4. In fact, the Kirkendall porosity should, unlikely, increase the molten slag physical infiltration. This aspect suggests that the castables' different microstructural features prevail in the slag-liquid interaction.

Fig. 5a presents the refractory microstructural profiles after firing at 1500 °C for 5 h, which indicates the samples' conditions before the slag attack, showing different CA_6 distributions: widely spread both in the matrix and at tabular alumina aggregates for the *in situ* spinel-forming castable, and only in the castable matrix for the pre-formed spinel-containing one. In order to better understand this aspect, an evaluation related to the initial step of calcium hexaluminate formation was carried out by analyzing the castables' micrographs at lower firing temperatures. Fig. 5b presents these micrographs attained from samples fired at 1300 °C for 5 h in areas where the presence of the precursor phase (CA_2) was more noticeable.

Based on these images, similar features for both castables are noticed: the presence of a liquid phase dissolving the fine tabular alumina particles, the CA_2 grains and the spinel crystals (the pre-formed ones, for the $MgAl_2O_4$-containing castables, and the *in situ* spinel which was already generated at

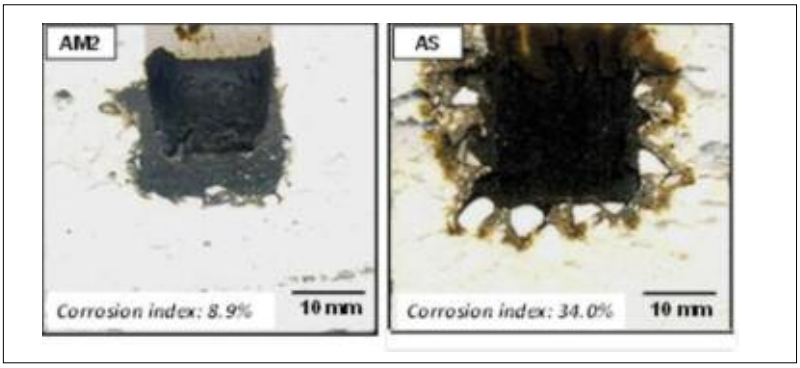

Fig. 4 Cross sections and corrosion indexes of the samples containing *in situ* and pre-formed spinel after the corrosion tests

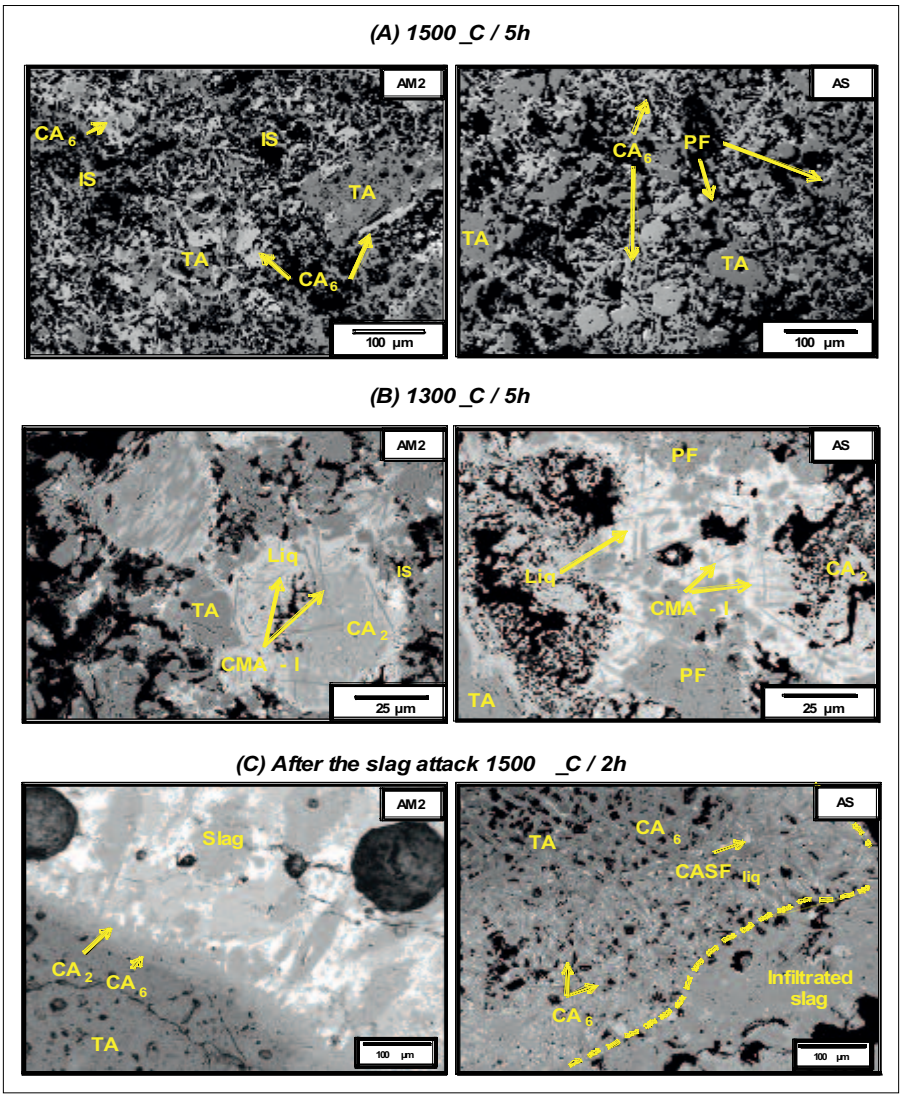

Fig. 5 Microstructure of AM2 and AS castables fired at 1500 °C/5 h (A) and 1300 °C/5 h (B), and after the corrosion tests at 1500 °C/5 h (C). TA: tabular alumina; IS: *in situ* spinel; PF: pre-formed spinel

this temperature, for the $MgAl_2O_4$-forming castable). The presence of acicular crystals precipitating out of the liquid can also be detected at 1300 °C. These crystals, which seemed to be CA_6 grains, were actually comprised by a ternary phase from the CaO-MgO-Al_2O_3 system, named CM_2A_8 (denoted hereafter as CMA-I). The preferential precipitation of this phase instead of CA_6 is mainly due to the MgO presence in liquid. Magnesia is incorporated into the liquid due to the dissolution of the spinel crystals, as can be seen in both images at 1300 °C in Fig. 5.

Additionally, according to thermodynamics calculations, the CMA-I generation is more favorable than the CA_6 one, as it presents more negative values of *Gibbs* free energy of formation for the whole temperature range. In Fig. 5, CMA-I was observed at 1300 °C, whereas CA_6 could be detected at 1500 °C, which indicates that a phase transition took place following the CMA-I → CA_6 direction. In fact, in the presence of MgO, CMA-I is preferentially formed and CA_6 is further generated via an indirect reaction involving the CMA-I decomposition firstly into CMA-II ($C_2M_2A_{14}$), plus MA and a liquid phase.

Afterwards, CMA-II melts incongruently, giving rise to CA_6, and again MA and liquid, suggesting that the CA_6 formation is necessarily preceded by the CMA phases and their decomposition. It is important to highlight that the melting points of the CMA phases are close to 1850 °C, which is clearly higher than the maximum temperature at which the castables were thermally treated. Nonetheless, the above-mentioned sequence indicates the likely trend of the CMA phases' decomposition into CA_6, due to the presence of liquid. According to the EDS results, the CMA-I crystals in Fig. 5b did not present a single chemical composition due to the presence of certain contents of Na_2O and SiO_2 as impurities, which might have helped to decrease the above-mentioned reaction temperatures.

Therefore, as the CA_6 generation mechanism in those refractories involves the precursor (CMA-I) precipitation, the distribution of this phase through the microstructure is associated with the previous location of the MgO sources. For the AM2 castable, the faster Mg^{2+} diffusion led to the spinel formation all over the microstructure, including at the edges of coarse tabular alumina aggregates. Hence, the broad distribution of CA_6 in this castable (as seen in Fig. 5a) is most likely related to this previous *in situ* spinel distribution. On the other hand, for the AS cast-able, the addition of the magnesium-aluminate was carried out in the matrix, and, as a consequence, this was the region where the CA_6 formation took place.

In order to analyze the effects of these different microstructural aspects on the castables´ corrosion resistance, SEM images were obtained after the corrosion cup-test experiments (Fig. 5c). Two mechanisms are proposed to explain the corrosion of the castables based on the different methods of spinel incorporation. For the *in situ* spinel-forming castable, the tabular alumina aggregates were mostly coated by a CA_6 layer, as shown in Fig. 5a, and thus the alumina availability for the reaction with the slag was reduced, resulting in the crystallization of a dense and compact second layer of CA_2, which protected the aggregate from further infiltrations. Conversely, the tabular alumina aggregates in the pre-formed spinel containing castable did not present any CA_6 protective layer (Fig. 5a). Hence, when the molten slag interacted with those aggregates, a higher amount of CA_6 crystals was generated, owing to the high alumina availability. As its formation is followed by a volumetric expansion ($\Delta V = 3{,}1$ %), cracks were detected in the aggregates as a result of these

uncontrolled reactions, leading to a continuous slag penetration and chemical reactions. For this reason, the tabular alumina aggregates in the pre-formed spinel-containing castable were found fully reacted and coated with CA_6 crystals, as illustrated in Fig. 5c. Thus, the increasing open porosity of the castable containing pre-formed spinel during the experiment due to the exceeded CA_6 formation strongly spoiled the refractory performance.

4 Final remarks

Based on the two proposed questions related to cement-bonded refractory castables, the main remarks of the present work can be summarized as follows:

- The faster Mg^{2+} mobility seems to induce the Kirkendall effect during the *in situ* spinel formation. Measurements based on SEM images indicated that the average pore size of the sample containing MgO <45 µm (AM2) increased with the firing temperature. In addition, a relationship between the pore size after firing at 1500 °C and the magnesia grain size was also detected, suggesting that the Kirkendall effect is most likely the reason for the spinel reaction being followed by pore generation.
- The distinct corrosion resistance of spinel-forming and spinel-containing castables was actually a consequence of the complex CA_6 generation route explained above. The in-depth microstructural analysis showed that the previous spinel location ruled the CA_6 crystals distribution in the microstructure before the slag attack, affecting the physico-chemical interactions between the refractory and the molten slag during testing. The correct understanding of the castables' microstructural evolution was highlighted as a relevant tool to predict the slag-refractory interaction products and inhibit undesired failures due to corrosive wearing.

Acknowledgments

The authors are grateful to the *Federation for International Refractories Research and Education (FIRE)*, the Brazilian funding agencies and the industrial partners of this work, represented by *Dr E Zinngrebe* and *Dr S. R. van der Laan* (*Ceramic Research Centre, Tata Steel Europe*).

References

[1] Kobayashi, M.; et al.: Use of alumina-magnesia castables in steel ladle sidewalls. Taikabutsu Overseas **17** (1997) [3] 39–44

[2] Sako, E.Y.; et al.: Microsilica role in the CA6 formation in cement-bonded spinel refractory castables. J. of Mater. Processing Technol. **209** (2009) 5552–5557

[3] Wagner, C.: The mechanism of formation of ionic compounds of higher order (Doube salts, spinel, silicates). Z. Physik Chem. **B34** (1936) 209–316

[4] Carter, R.E.: Mechanism of solid-state reaction between magnesium oxide and aluminum oxide and between magnesium oxide and ferric oxide. J. Amer. Ceram. Soc. **44** (1961) [3] 116–120

[5] Nakagawa, Z.; et al.: Effect of corundum/periclase sizes on expansion behavior during synthesis of spinel. Proc. UNITECR'95, Kyoto, Japan (1995) 379–386

[6] Smigelskas, A.D.; Kirkendall, E.O.: Zinc diffusion in alpha brass. Trans. AIME **171** (1947) 130–142

[7] Braulio, M.A.L.; et al.: Basic slag attack of spinel-containing refractory castables. Ceramics Int. **37** (2011) [6] 1936–1945

[8] Zhang, S.; Lee, W.E.: Spinel-containing refractories. Refractories Handbook, EUA (2004) 215–258

[9] Braulio, M.A.L.; et al.: Expansion behavior of cement-bonded alumina-magnesia refractory castables. Amer. Ceram. Soc. Bulletin **86** (2007) [12] 9201–9206